*Sensors & Transducers, Vol. 255, Issue 1, January 2022, pp. 53-61*

**Sensors & Transducers**

Published by IFSA Publishing, S. L., 2022
http://www.sensorsportal.com

# Defected Ground Structures Tuned by MEMS Switches: Review

**[1, *] Nisha Jose K. and [2] Boby Philip**
[1] Department of EC, SCTCE, Trivandrum, India
[2] Division of EE, SCTCE, Trivandrum, India
[1] Tel.: 9446149873
E-mail: nisha@sctce.ac.in

*Received: 2 December 2022 Accepted: 14 January 2022 Published: 31 January 2022*

**Abstract:** This paper presents a review of the applications of Radio Frequency Micro electro mechanical (RFMEMS) switches for the tuning of Defected Ground Structures (DGS). In wideband communication systems, tunable systems are preferred over multichannel systems as they offer compactness. Microelectromechanical system (MEMS) based switches are replacing semiconductor based switches in tuning of RF devices such as filters, phase shifters, antennas etc. Defected Ground structures are employed as filters or as slow wave structures for achieving compactness for other filter designs. This review includes MEMS based tuning of Defected Ground Structure based filters over planar transmission lines such as CPW and microstrip transmission lines. Compared to microstrip based designs, CPW based DGS filters have ease of implementation with other coplanar elements, since it does not require via holes. MEMS DC contact switches are employed for inductive tuning by varying the effective area of DGS, while shunt switches are employed for the capacitive gap tuning. A large number of distributed MEMS switches over CPW line forms a Distributed MEMS Transmission Line (DMTL). DMTL based structures are also employed for tuning of DGS structures.

**Keywords:** Micro electro mechanical systems (MEMS), Defected Ground Structures (DGS), Distributed MEMS Transmission Lines (DMTL).

## 1. Introduction

Tuneable Filters based on defected ground structures have seen many important applications in communication systems in the past decade. Defected ground structures are characterised by a slow wave effect that results in circuit compaction, as well as a band stop effect that finds application in RF filters. Tunability is also employed for compacting multi-channel circuits. MEMS switches are increasingly replacing semiconductor switches for applications in tunable RFICsystems, due to their characteristics such as low insertion loss (I.L), low power consumption and high linearity. The only disadvantages of MEMS switches when compared to semiconductor devices are their comparatively larger rise times. This paper aims to review MEMS tuned DGS filters.

## 2. History of MEMS

Richard Feyman, spoke about storing information onto individual atoms, at his famous lecture at the annual meeting of the APS Society in 1959, 'There's Plenty of Room at the Bottom: An Invitation to Enter a New Field of Physics'[1]. Feyman also suggested manipulation of these atoms using machines at nanoscale. Deep Silicon etching was demonstrated in 1967 [2]. Micromechanical nozzles were developed for inkjet printer in 1979. Tanner et.al. developed the first micro engine based on surface micromachining at Sandia National Laboratories [3, 4]. A wide range of micro mechanical sensors and actuators have followed, in engineering, medicine and other fundamental sciences.

## 3. MEMS and RF MEMS

The application area of MEMS in RF communication systems, is known as RF MEMS. Frequencies of GHz, or wavelengths of $\mu m$ can be generated using micro electromechanical resonators. Q factors of such resonators are in the range of thousands, as compared to hundreds for than semiconductor-based devices. The low heat dissipation and ultra-small moment of inertia of MEMS devices leads to ultra-low power consumption in $nJ$, which is much less compared to $\mu J$ for semiconductor devices. Also, the on-state resistance, of MEMS devices are low $(1-2\Omega)$, leading to low insertion loss.

## 4. Characteristics of RF MEMS Switches

MEMS switches are characterised by low insertion loss $(I.L)$ and high isolation. $I.L$ for shunt switch is typically better than $-0.04$, and for series switch $-0.1dB$. Isolation for shunt switch is better than $-60dB$ at 5 to $100GHz$ whereas power consumption is in $nJ$. In comparison, semiconductor /PIN switches have higher insertion loss $-1\ dB$ and very low isolation (near $-5dB$) at RF frequencies. MEMS switches suffer from larger rise times ($\mu s$ as compared to $ns$) in place of semiconductor switches, which can limit its use in mission critical applications such as airborne applications and satellite systems.

A disadvantage of MEMS switch is low power handling under hot switching (typically up to 30dBm or $1W$). MEMS switches with higher power handling upto $40dBm$ (or $10W$) has been developed [5]. MEMS switches with $3.6W$ of power handling and monolithically integrated with GaN MMIC is discussed in [6].

Reliability of MEMS switches is typically about $10\ to\ 60$ billion cycles. On-board satellite systems and air borne applications require reliability over 100 billion cycles. A MEMS DC contact switch with capping technique has reported 200 billion lifecycles at 10W cold switched RF power [5]. Raytheon demonstrated capacitive switches with reliability of 100 billion cycles and power handling of $30dBm$ [7]. Practical solutions to reliability issues in MEMS is discussed in [8]. MEMS switches usually require higher control voltages than PIN diode switches. Actuation voltages typically vary from 20 to 80V. This can be reduced using Distributed MEMS transmission lines (DMTL).

MEMS switches and relays are employed for tuning RFICs. MEMS relays can tune the lengths of evanescent cavities [9] and optical laser cavities [10]. MEMS switches are employed in choosing between transmission paths in phase shifters or for reconfigurable circuits [11, 12]. A transmission line can be short or open circuited by loading MEMS metal beams. Varactors based on MEMS shunt switches use analog actuation voltages [13-15].

## 5. Defected Ground Structures

Etched defects in the ground plane of a transmission line gives rise to a Defected Ground Structure (DGS) [16 to 29]. The equivalent inductive and capacitive elements of the defect can be varied using MEMS switches using MEMS DC contact switches and MEMS shunt switches, as discussed below.

## 6. Tuning Defected Ground Structures using MEMS Switches

### 6.1. Using MEMS Switches Across the Gaps of DGS

The field coupling into the defect is tuned to vary the equivalent capacitance. In [30], MEMS DC contact fixed - fixed beam switches placed over periodic defects are employed as stubs for impedance matching, as shown in Fig. 1.

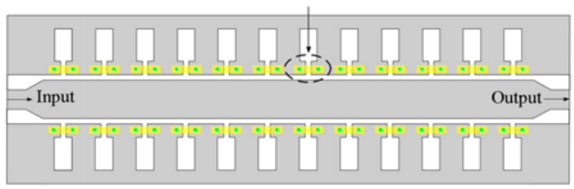


(a)

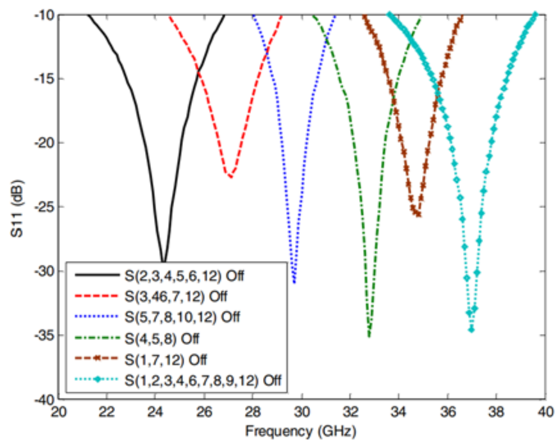


(b)

**Fig. 1.** (a) Capacitive tuning by loading MEMS switches across the gaps of DGS; (b) R.L. for different switching states, [30].

The switch beams when actuated short out the defect gaps, to eliminate the slow wave effect of the defect. The measured results demonstrate wide coverage of the Smith chart, as shown in Fig. 2, with a maximum VSWR of 12:1 at 60 GHz. The measured loss of the network when used to match a 10 Ω load to 50 Ω from 22 GHz up to 40 GHz is only -0.5 dB.

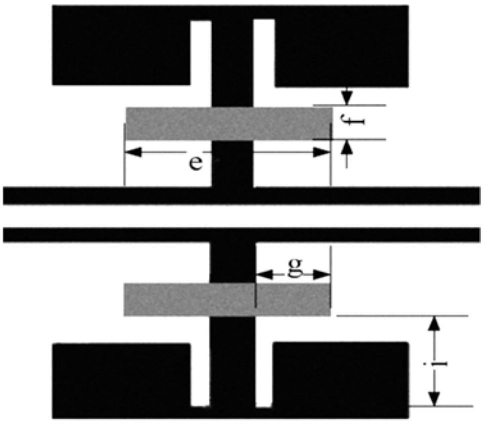


(a)

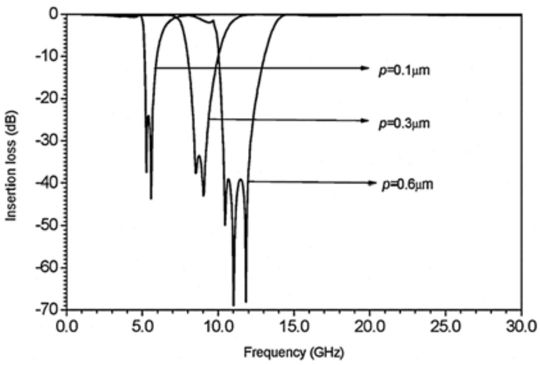


(b)

**Fig. 2.** (a) Capacitive tuning by loading MEMS switches (shown in grey) across the gaps of a T shaped DGS (shown in black (b)). Variation in resonant frequency [31].

MEMS switches placed across the gaps of DGS are employed in tuning of resonant frequency in filters. [31]. The field coupling into the defect is affected by the presence of the switch beam, varying the inductance. The switch anchors are raised above ground level while the actuation electrode is situated below ground level, to avoid pull in of the switches.

Capacitive tuning method results in nonlinear variation of resonant frequency with beam height, such that lowest beam heights, result in maximum variation, see Table 1. In this method, the depth of attenuation also reduces with the beam height.

**Table 1.** MEMS switches across DGS gaps- tuning of filter parameters [31].

| Switch height p(µm) | 20 dB BW (GHz) | Centre frequency $f_o$ (GHz) | I.L (dB) | R.L (dB) |
|---|---|---|---|---|
| 0.6 | 2.2 | 12 | -40 | -0.3 |
| 0.3 | 1.6 | 8.8 | -35 | -0.3 |
| 0.1 | 1 | 5.2 | -30 | -0.3 |

A Defected ground structure with slots performs as a BSF and with MEMS switches across the gaps it functions as a hybrid resonator. The shunt capacitance is a function of MEMS switch height [32, 33]. The actuation voltages to the switches are varied from 0 to 44 V, to vary the filter parameters as shown in Table 2.

**Table 2.** MEMS tuning of CPW DGS filter [32].

| Bias voltage (V) | 0 | 13 | 23 | 33 | 44 |
|---|---|---|---|---|---|
| Centre frequency (GHz) | 12.3 | 11.8 | 11.2 | 9.8 | 8.5 |
| 3 dB Bandwidth (GHz) | 4 | 3.5 | 3.1 | 2.6 | 2.1 |
| Return loss (dB) | 2.3 | 2.4 | 2.5 | 2.6 | 2.8 |

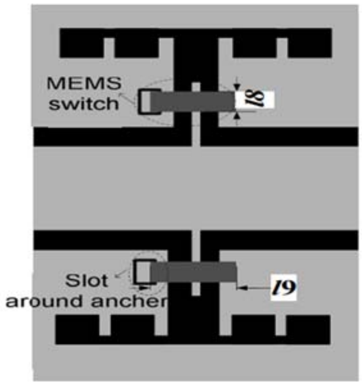


(a)

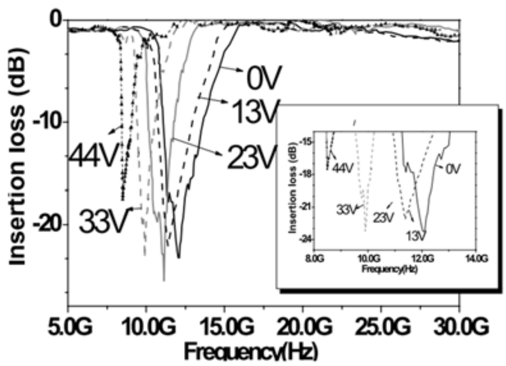


(b)

**Fig. 3.** (a). CPW TDGS with four slots and tuned by MEMS switches across gaps. (b). Variation of resonant frequency with actuation voltage [32].

## 6.2. Using MEMS DC Contact Switches Over the Inductive Defects of DGS

The current loop inside the defect and its equivalent inductance, can be varied by placing DC contact switches to short out defect regions. In comparison to semiconductor switches, usage of

MEMS switches achieve reduction in insertion loss, power consumption and increase in linearity. At lower frequencies, where the circuit dimensions are larger, MEMS switches are replaced by semiconductor switches.

MEMS series DC contact switches are employed to vary the dimension of a square DGS. The change in equivalent inductance varies the resonant frequency and the cut off frequency [34], as shown in Fig. 4 a, b. The resonant frequency of the basic cell increases from 20.3 GHz to 23.44 GHz due to decrease in the effective area. The filter consists of 3unit cells in cascade and resonant frequency varies from 23.4 to 18.2 GHz. The cascaded filter has wider bandwidth than the unit cell.

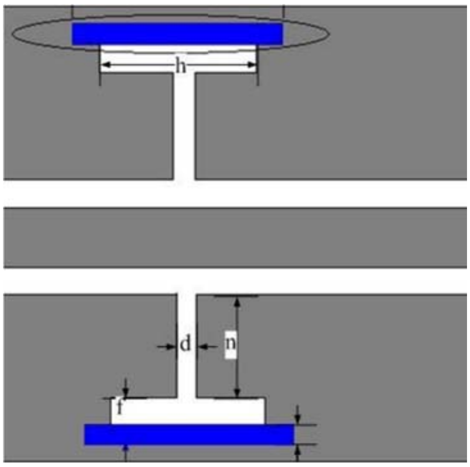


(a)

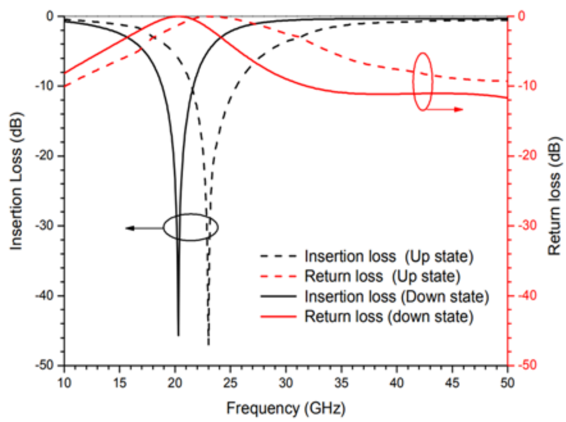


(b)

**Fig. 4.** (a). MEMS switches (marked in blue) loaded over defect area; (b) Frequency shift due to actuation [34].

DGS structures that are periodic in two dimensions have a constant equivalent capacitance while the inductance varies with the number of cells [35]. A 2D periodic DGS is reconfigured by RF MEMS series switches of fixed- fixed type [36]. The respective number of tuning states obtained is 2 and 8 for [35] and [36].

A narrow slot that interconnects two defect regions is loaded with MEMS switches. This results in two tuning states for a reconfigurable filter [37], see Fig. 5. Actuation of the switch eliminates the effect of the second region. By actuating MEMS switch, the reconfigurable frequency response switches from bandpass to band stop response. In [38], a microstrip antenna having a defect slot etched in the ground plane is tuned using MEMS series switches. This eliminates the effect of the slot line region succeeding the switch, and creates 3 tuneable frequency states [38].

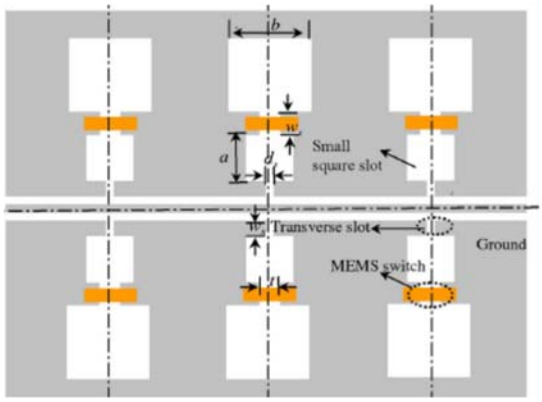


(a)

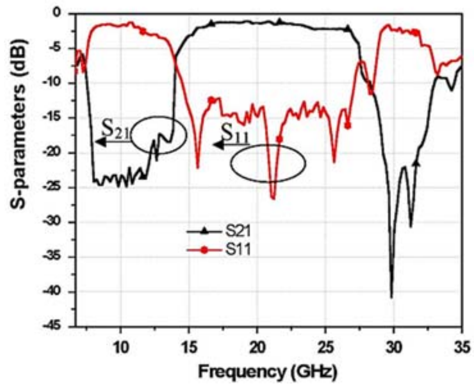


(b)

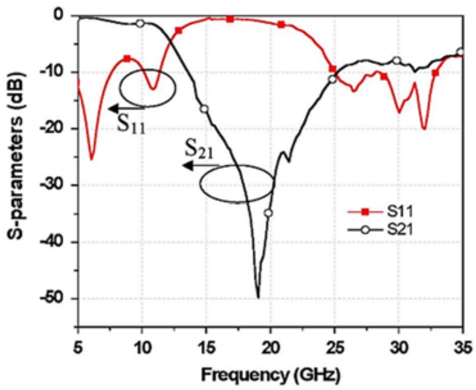


(c)

**Fig. 5.** (a) MEMS switches for reconfiguring the effective defect structure, (b) OFF state of switch, bandpass filter. (c) ON state of switch, bandstop filter [36].

MEMS switches are employed in a microstrip DGS at different positions, for a reconfigurable frequency response [39]. Multiple contact MEMS switches are loaded over a DGS [40]. In most of these works, attenuation depth is greater than $20\ dB$, while insertion loss varies from filter to filter, but losses are generally lesser at low frequencies ($< -1\ dB$) than higher frequencies ($-2$ to$-3\ dB$). A comparative study of the MEMS based tunable filters is given in Table 3.

DGS filters are characterised by Q factors that vary according to defect shape. Prior to DGS structures, Photonic Band gap structures (PBG) (see Appendix B) were generally employed, having shapes such as triangular, square etc. But Photonic band gap structures had frequency responses primarily decided by other parameters such as periodicity filling factor, etc. and was less dependent on shape of the lattice [41]. For DGS, the band stop properties result from the combined effect of capacitive gap and inductive aperture. Hence the frequency response is dependent on both the dimensions and the shape of the defect [42].

A spiral DGS can achieve large Q and high rejection, with compact area. The large loop length resulting from the spiral structure creates large inductance. But it does not allow for the positioning of anchors of MEMS switches. Periodic structures such as fractal DGS [44], are efficient and compact, but these structures also are not convenient for loading MEMS switches. Other reported DGS shapes include circular [45], alphanumeric [46], H [47, 48] and U shape [49] and interdigital DGS [50]. The alphanumeric DGSs and the circular DGS have low loop lengths and large area. Hence switch actuation changes the shape of the defect, rather than its dimensions and hence the change in the resulting frequency response cannot be easily predicted. The U DGS has very narrow bandwidth or high Q.

The interdigital DGS [50] has acceptable rejection and moderate bandwidth. The loop length is large, creating a larger tuning range of resonant frequency, in a predictable manner. Even though the structure of the interdigital DGS is compact, it is suitable to be tuned by MEMS switches. T shaped DGS [51] includes protruding metal strips, and provides a large gap capacitance. The T shaped structure is convenient for placing switch anchors.

## 6.3. Using Distributed MEMS Transmission Lines

A third method of tuning DGS structures employs distributed MEMS switches, called Distributed MEMS Transmission Lines (DMTL) between adjacent DGS structures [52]. The capacitance of the MEMS switches is controlled through electrostatic actuation, and varies the effective electrical length between DGS structures. When compared to designs employing independent MEMS switches, DMTL based designs allow switches to be operated at lower actuation voltages, by compensating for the upstate switch capacitances.

## 6.4. Using a Combination of the above Methods

In [54], MEMS switches are employed for tuning both the resonant frequency as well as bandwidth of a T shaped DGS as in Fig. 6.a. MEMS ohmic switches (or DC contact switches) are fixed over four branches of a T -DGS, for fine tuning of resonant frequency. MEMS series switches placed across the gaps of the DGS are used for coarse tuning. Bandwidth is tuned using distributed MEMS switches in a DMTL.

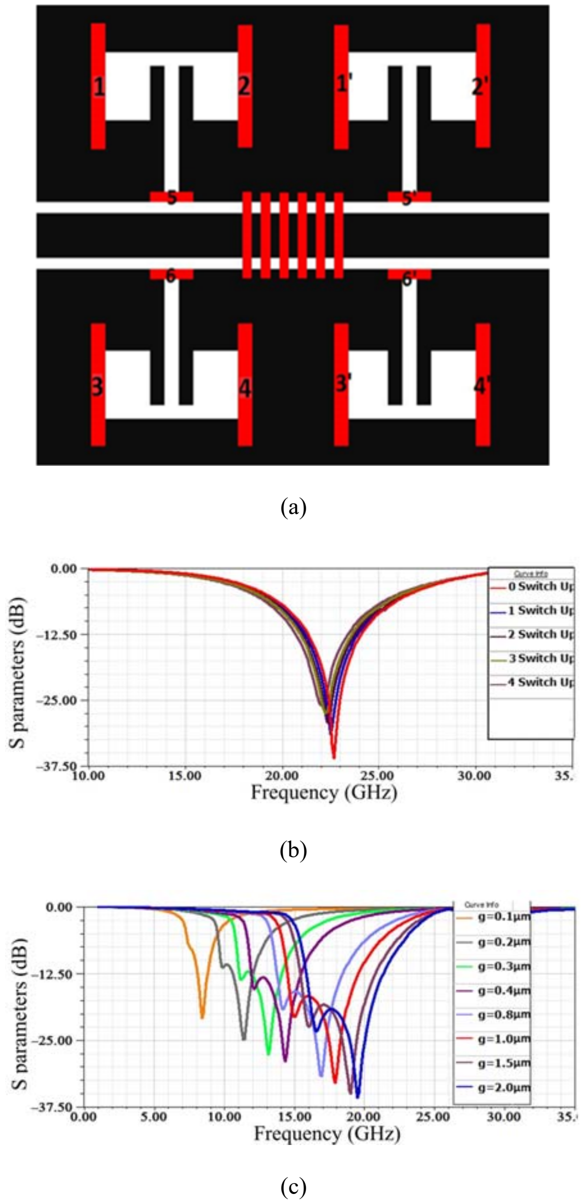


**Fig. 6.** (a) BSF filter with tunable resonant frequency and bandwidth, using T-DGS and MEMS switches, (b) Fine Tuning using DC contact switches (1 to 4) & (1' to 4') c. Coarse tuning using MEMS switches over DGS gaps [54].

The fine-tuning methods increases the resonant frequency from $22\ to\ 22.8\ GHz$, see Fig. 6.b. The depth of the attenuation null and the resonant frequency are slightly shifted due to the presence of switch beams in the upstate.

Coarse tuning of resonant frequency is achieved by providing actuation voltages to MEMS switches placed across the gaps of DGS structures, switches 5, 6 and 5', 6'of Fig. 6a. The variation of resonant frequency in height of the switch beam results in nonlinear variation of the resonant frequency as shown in Fig. 6.c. Maximum variation is obtained in resonant frequency occurs for extremely small beam heights of less than 0.1μm. By placing the actuation electrode below ground level, pull down is avoided. The resonant frequency corresponding to the upstate of the gap tuning switch is 20 GHz. For a gap height of 0.1μm, it reduces to 8.4 GHz.

In [55], an interdigital DGS is tuned using MEMS DC contact switches loaded at the bends. Actuation of the switch short out the effect of the defect region after the bend. Additional switches allow large number of tuning states. The filter and its tunable frequency response is shown in Fig. 7 a, b. For the filter with switches only at the bends, the resonant frequencies are non-uniformly spaced. With large number of additional switches, closely spaced resonant frequencies are obtained, while variation in attenuation depth is only $3dB$, between $-23$ to $-26dB$.

A quarter wave comb-line resonator etched on the signal strip of a CPW line, on a high resistivity silicon (HRS) substrate, is tuned using MEMS switches [56]. DGS is employed to reduce the filter dimensions and increase the quality factor. The dimensions of the defect structure are optimised through equivalent circuit simulations in Ansoft HFSS. The filter has an I.L. of - 0.51 dB and -2 dB respectively, for up and down states of the MEMS switches. In the stopband, R.L. varies between -0.3 to -0.5dB. The filter achieves a tuning range from 29.8–35.6 GHz and rejection between 37 and 45 dB, while the maximum with actuation voltage of the MEMS switches is 44.5 V.

A comparative study of the MEMS based tunable filters is given in Table 3. It is seen that MEMS switches are an excellent choice for achieving tuning in RF communication systems.

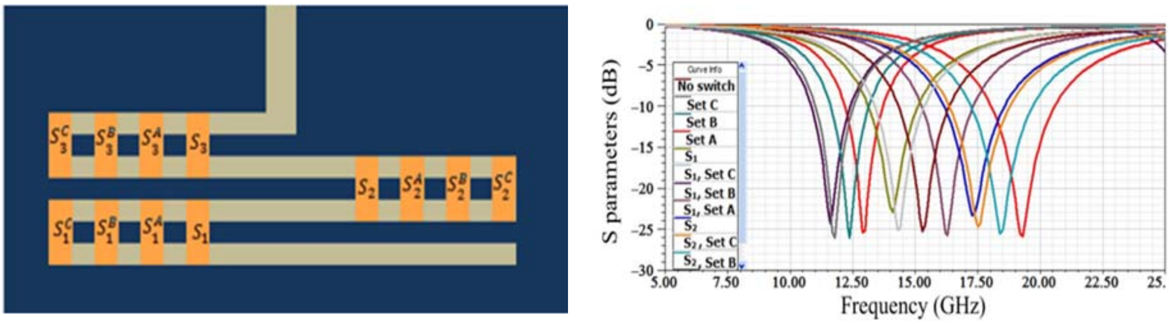


(a) (b)

**Fig. 7.** a) Tunable interdigital DGS using MEMS DC contact switches over bends, b) frequency response showing large number of resonant frequencies [55].

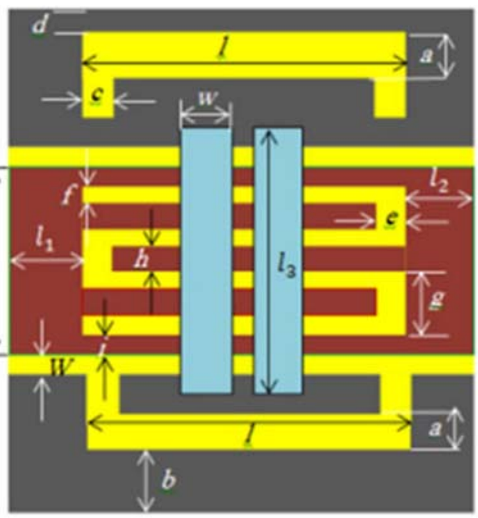

**Fig. 8.** CPW combline quarter wave resonator loaded with MEMS switches [56].

**Table 3.** Comparison of DGS filters tuned using MEMS.

| Sl. No | Frequency (GHz) | Band width (GHz) | Rejection (dB) | I.L Pass band (dB) | R.L Stop band (dB) | Actuation Voltage (V) |
|---|---|---|---|---|---|---|
| 1. [31] BSF | 5 to 15 | 2- 1 (20 dB) | -30 | -2* | -.5 | --- |
| 2. [32] BSF | 8.5 to 12.3 | 2.1-3.5 (3 dB) | -15 to -20 | -2* | -2.3 to -2.8 | 44 |
| 3. [33] BPF | 10 to 13.5 | --- | -15 to -20 | -2.3 to -3.1 | -.7* | 33 |
| 4. [34] BSF | 18.2 to 23.4 | 2.87 to --- | -32 to -35 | -1 to -2* | -.5 | ---- |
| 5. [35] BSF | 19-27 GHz | 8.1(3dB) | -22 to -18 | -0.1 to -2.5 | -0.5 | 20 |
| 6. [36] BPF | BPF (20.1)- BSF (19.8) | 9.6-9.2 (3 dB) | -25 to -50 | -1.55 to -1.2 | -2.5 to -1 | 38 |
| 7. [37] BPF | 1.62 to 1.85 | 0.13 (3 dB) | -20* | -1.3 to -2.9 | --- | |
| 8. [38] LPF | 0 (LPF) | 8.2 to 25.2 | -20* | -2* | -1.2 to -1.3 | 33 |
| 9. [54] BSF | 8.4 to 20 | 10 to 19 (3 dB) | -20 to -47 | -0.15 to -1.95 (-1.05 avg.) | -0.4 | 4.5, 5, 10 |
| 10. [55] BSF | 11.6-19.5 | 5 to 6.5 | -23 to -26 | -4 to -1.1 | -0.3 | 9.5 |
| 11. [56] BSF | 29.8–35.6 | ------ | -35 to -45 | -0.15 to -2 | -0.3 to -0.5 | 44.5 |

Note: values denoted by * indicate that the values are obtained from graphs through visual observation

## 7. Conclusion

MEMS switches are employed for the tuning and reconfiguring of DGS structures for varying the resonant and cut off frequencies of the filter. The switches are employed for capacitive or inductive tuning, or both. Inductive tuning results from tuning the structure and dimensions of DGS. Capacitive tuning is achieved by altering the field coupling into the defect structure. The spacing between adjacent DGS structures can be altered using distributed MEMS switches, to vary the filter bandwidth. MEMS devices are characterised by very low power consumption and low insertion loss and as well as high linearity, as compared to semiconductor switches. The only disadvantage of MEMS switches is the larger rise times required for mechanical switching, which might be of importance in mission critical applications or air borne applications.

## References


[1]. Richard P. Feynman, There's Plenty of Room at the Bottom, *Engineering and Science Caltech Magazine*, Feb 1960, pp. 22-36.

[2]. Waggener, H. A., Electrochemically controlled thinning of silicon, *The Bell System Technical Journal,* 49, 3, 1970, pp. 473-475.

[3]. Tanner, Danelle M., Norman F. Smith, and Duane J. Bowman, First reliability test of a surface micromachined microengine using ShiMMeR. No. SAND-97-0746C; CONF-970968-5, *Sandia National Labs*., Albuquerque, US, 1997, pp. 14-23.

[4]. Petersen, Kurt E. Silicon as a mechanical material, *Proceedings of the IEEE*, 70, 5, 1982, pp. 420-457.

[5]. John Maciel, Sumit Majumder, James Lampen and Charles Guthy, Rugged and Reliable Ohmic MEMS Switches, in *Proceedings of the IEEE MTT-S Int. Microw. Symp. Dig.,* 2012, pp. 1-3.

[6]. Mohamed, AM Mahmoud, et al., High power GaN monolithically integrated RF MEMS switches, in *Proceedings of the IEEE Microwave Integrated Circuits Conference (EuMIC),* 2013, pp. 348-351.

[7]. Alex Grichener, and Gabriel M. Rebeiz, High-Reliability RF-MEMS Switched Capacitors with Digital and Analog Tuning Characteristics, *IEEE Trans. Microw. Theory Tech.,* Vol. 58, No. 10, Oct. 2010, pp. 2692-2695.

[8]. Huang, Yunhan, et al., MEMS reliability review, *IEEE Transactions on Device and Materials Reliability,* Vol 12. No. 2. 2012, pp. 482-493.

[9]. Park, Sang-June, Isak Reines, Chirag Patel, and Gabriel M. Rebeiz. High-Q RF-MEMS 4–6-GHz tunable evanescent-mode cavity filter, *IEEE Transactions on Microwave Theory and Techniques,* Vol. 58, No. 2, 2010, pp. 381-389.

[10]. Liu, A. Q., and X. M. Zhang, A review of MEMS external-cavity tunable lasers, *Journal of Micromechanics and Microengineering,* Vol. 17, No. 1, 2006, pp. R1-R13.

[11]. M. Kim, B. Hacker, R. E. Mihailovich, and J. F. DeNatale, A DC-to-40 GHz Four-Bit RF MEMS True-Time Delay Network, *IEEE Microw. Wireless Comp. Lett.,* Vol. 11, No. 2, 2001, pp. 56-58.

[12]. Arnaud Pothier, Jean-Christophe Orlianges, Guizhen Zheng, Corinne Champeaux, Alain Catherinot, Dominique Cros, Pierre Blondy, and John Papapolymerou, Low-Loss 2-Bit Tunable Bandpass Filters Using MEMS DC Contact Switches, *IEEE Trans. Microw. Theory Techn,* Vol. 53, No. 1, 2005, pp. 354-360.

[13]. RF MEMS: Theory, Design, and Technology Gabriel M. Rebeiz. *John Wiley and Sons*, 2001.

[14]. C. L. Goldsmith, Z. Yao, S. Eshelman, and D. Denniston, Performance of low-loss RF MEMS

capacitive switches, *IEEE Microwave Guided Wave Lett.,* Vol. 8, Aug. 1998, pp. 269-271.

[15]. G. M. Rebeiz, and J. B. Muldavin, RF MEMS switches and switch circuits, *Microw. Mag.,* Vol. 1, Dec 2001, pp. 59–71.

[16]. L. H. Weng, Y. C. Guo, X. W. Shi, and X. Q. Chen, An Overview On Defected Ground Structure, *Progress in Electromagnetics Research B,* Vol. 7, 2008, pp. 173–189.

[17]. G. Breed, An Introduction to Defected Ground Structures in Microstrip Circuits, *High Frequency Electronics,* 2008, pp. 50-54.

[18]. Yablonovitch, Eli, Inhibited spontaneous emission in solid-state physics and electronics, *Physical Review Letters,* 58, 20, 1987, pp. 2059-2062.

[19]. John, S., Strong localization of photons in certain disordered dielectric superlattices, *Phys. Rev. B,* Vol. 58, No. 23, 1987, pp. 2486–2489.

[20]. John D. Joannapoulos, Photonic Crystals: Molding the flow of light, 2nd ed., *Princeton University Press*, 2013.

[21]. C. M. Soukoulis, The History and Review of the Modelling and Fabrication of Photonic Crystals, *Nanotechnology,* 13, 2002, pp. 420-423.

[22]. Y. Qian, V. Radisic, and T. Itoh, Simulation and experiment of photonic band-gap structures for microstrip circuits, in *Proceedings of the APMC'97*, Hong Kong, Dec. 1997, pp. 585-588.

[23]. Radisic, Y. Qian, and T. Itoh, Broad-band power amplifier integrated with slot antenna and novel harmonic tuning structure, in *Proceedings of IEEE MTT-S. Symp. Dig.,* Baltimore, MD, June 7–12, 1998, pp. 1895–1898.

[24]. Radisic, V., Y. Qian, R. Coccioli, and T. Itoh, Novel 2-D photonic bandgap structure for microstrip lines, *IEEE Microwave and Guided Wave Letters,* Vol. 8, No. 2, Feb 1998, pp. 69–71.

[25]. Horii, Y. and M. Tsutsumi, Harmonic control by photonic band gap on microstrip patch antenna, *IEEE Microwave and Guided Wave Letters,* Vol. 9, Jan 1999, pp. 13–14.

[26]. Ian Rumsey, Melinda Piket-May, and P. Keith Kelly, Photonic Bandgap Structures Used as Filters in Microstrip Circuits, *IEEE Microwave Guided Wave Lett.,* Vol. 8, No. 10, Oct. 1998, pp. 336-338.

[27]. Qiang, R., Y. Wang, and D. Chen, A novel microstrip bandpass filter with two cascaded PBG structures, *2001 IEEE AP-S Digest*, 2001, pp. 510–513.

[28]. Vesna Radisic, Yongxi Qian, Member, Broad-Band Power Amplifier Using Dielectric Photonic Bandgap Structure, *IEEE Microwave Guided Wave Lett.,* Vol. 8, No. 1, Jan 1998, pp. 13-14.

[29]. C.-S. Kim, J.-S. Park, D. Ahn, and J.-B. Lim, 1-D periodic defected ground structure for planar circuits, *IEEE Microwave Guided Wave Lett.,* April 2000, pp. 131 – 133.

[30]. S. Fouladi, A. Akhavan Fomani, and R. R. Mansour, A Novel Reconfigurable Impedance Matching Network Using DGS and MEMS Switches for Millimeter-Wave Applications, *Microwave Symposium Digest, IEEE MTT-S Int.,* 2008, pp. 145-148.

[31]. Z. L. Deng, N. B. Zhang, and J.-M. Huang, A Tunable Ultra-wide band Band-stop Filter Based on EBG Structures Using MEMS Technology, in *Proceedings of the IEEE International Conference on Mechatronics and Automation,* Changchun, China, 2009, pp. 3579-3583.

[32]. Zhang, N., Z. Deng, and F. Sen, CPW tunable band-stop filter using hybrid resonator and employing RF MEMS capacitors, *IEEE Trans. on Electron Devices,* Vol. 60, No. 8, 2013, pp. 2648-2655.

[33]. Nai-Bo Zhang, Zhong-Liang Deng, and Ming-Yu Zhao, A Novel Tunable Band-stop Filter based on RF MEMS Technology, *in Proceedings of the International Conference on Computer, Mechatronics, Control and Electronic Engineering (CMCE)*, Vol. 6, 24-26 Aug. 2010, pp. 1-4.

[34]. J. -M. Huang, F. Zhu and Z. L. Deng, A Novel Design of Tunable Band-Stop Filter Using MEMS Technology' in *Proceedings of the IEEE International Conference on Wireless Communications, Networking and Mobile Computing,* 2009, pp. 1-3.

[35]. Hamad, Ehab KI, Amr ME Safwat, and Abbas S. Omar, 2D periodic defected ground structure for coplanar waveguide' in *Proceedings of the German Microwave Conference (GeMiC' 2005)*, 2005, pp. 25-28.

[36]. Ehab K. I. Hamad, Amr M. E. Safwat, Abbas S. Omar, A MEMS Reconfigurable DGS Resonator for K-Band Applications, *Journal of Microelectromechanical Systems,* Vol. 15, No. 4, August 2006, pp. 756 -762.

[37]. Muhammad Faeyz Karim, Ai-Qun Liu, A. Alphones, and Aibin Yu, A Reconfigurable Micromachined Switching Filter Using Periodic Structures, *IEEE Trans. Microw. Theory Tech.,* Vol. 55, No. 6, June 2007, pp. 1154 -1162

[38]. Chon Chio Leong, Ka Fai Chang, Wai Wa Choi, and Kam Weng Tam, Tunable Defected Ground Structure and its Applications to Simultaneous Reconfigurable Communication and Partial Discharge Detection, in *Proceedings of the IEEE Conference on Antennas and Propogation,* 2012, pp. 159-160.

[39]. S. Ur Rehman , A. F. A. Sheta & M. A. S. Alkanhal, Compact MEMS Based Reconfigurable Bandpass Microstrip Filter Using Defected Ground Structure (DGS), *Journal of Electromagnetic Waves and Applications*, 26, 2-3, 2012, pp. 353-365.

[40]. X.L. Guo, C. Xu, G.A. Zhang, Z. J. Zhang, H.H. Yin, Z.L. Wang, Tunable low-pass MEMS filter using defected ground structures (DGS), *Solid-State Electronics,* 94, 2014, pp. 28–3.

[41]. Y. Qian, V. Radisic, and T. Itoh, Simulation and experiment of photonic band-gap structures for microstrip circuits, *in Proceedings of the APMC'97*, Hong Kong, Dec. 1997, pp. 585-588.

[42]. Hamad, E. K. I., Safwat, A. M. E., and Omar, A. S.: L-shaped defected ground structure for coplanar waveguide, in *Proceedings of IEEE the AP-S Int. Symp. And USNC/URSI National Radio Science Meeting,* Washington DC, July 2005, pp. 663-666.

[43]. C.-S. Kim, J.-S. Lim, S. Nam, K.-Y. Kang, and D. Ahn, Equivalent circuit modeling of spiral ground structure for microstrip line, *IEEE Electron. Lett.,* Vol. 38, 2002, pp. 1109–1110.

[44]. Martin Kufa, Zbyněk Raida, Comparison of Planar Fractal Filters on Defected Ground Substrate, *Radioengineering*, Vol. 21, No. 4, December 2012, pp. 1019-1024.

[45]. A. B. A. Rahman, A. K. Verma, A. Boutejdar, and A. S. Omar, Control of bandstop response of Hi-Lo microstrip low-pass filter using defect in ground plane,

*IEEE Trans. Microw. Theory Tech.*, Vol. 52, No. 3, Mar. 2004, pp. 1008–1013.

[46]. Amr M. E Safwat, Letter-shaped microstrip ground defects, *International Journal of Microwave and Wireless Technologies,* 4, 5, 2012, pp. 523–528.

[47]. Mrinal Kanti Mandal and Subrata Sanyal, A Novel Defected Ground Structure for Planar Circuits, *IEEE Microwave And Wireless Components Letters*, Vol. 16, No. 2, February 2006, pp. 93-96.

[48]. B. Boutejdar, A., Amari, S., Elsherbini, A., Omar, A. S., A novel low pass filter with ultra-wide stopband and improved Q-factor performance using H-defected ground structure (DGS), in *Proceedings of IEEE AP-S/USNC/URSI National Radio Science Int. Symp.*, Honolulu, HI, USA, 2007, pp. 1545-1548.

[49]. Boutejdar, A.; Batmanov, A., Awida, M. H., Burte, E. P., Omar, A., Design of a new bandpass filter with sharp transition band using multilayer-technique and U-defected ground structure, *IET Microw., Antennas Propag.,* 4, 2010, pp. 1415–1420.

[50]. Atallah Balalem, Ali R. Ali, Jan Machac, Senior Member, IEEE, and Abbas Omar, Fellow, IEEE, Quasi-Elliptic Microstrip Low-Pass Filters Using an Interdigital DGS, *IEEE Microw. Comp Lett.,* Vol. 17, No. 8, Aug. 2007, pp. 586-588.

[51]. M. Kim and B. Lee, Analysis and synthesis of defected ground structures (DGS) using transmission line theory, in *Proceedings of Eur. Microw. Conf.*, Oct. 2005, pp. 397–400.

[52]. Karim, M. F., Liu, A.-Q., Alphones, MEMS-Based Tunable Bandstop Filter Using Electromagnetic Bandgap (EBG) Structures, in *Proceedings of the Asia-Pacific Microwave Conf.,* 3, 2005, p. 4.

[53]. Khandelwal, M. K., Kanaujia, B. K., & Kumar, S., Defected ground structure: fundamentals, analysis, and applications in modern wireless trends, *Hindawi International Journal of Antennas and Propagation*, 2017, pp. 1-22.

[54]. K. Nisha Jose, M. R. Baiju, A tunable band stop filter using T shaped DGS and MEMS switches on CPW, *Perspectives in Science*, Vol. 8, 2016, pp 505-509.

[55]. Nisha Jose K., V. Suresh Babu, Baiju M. R., A Tunable band stop filter for Ku band communication systems using DGS and MEMS switches, *Sensors & Transducers Journal,* Vol. 232, Issue 4, 2019, pp. 15-18.

[56]. Mirebrahimi, S. M., Dousti, M., & Afrang, S, High-Q CPW tunable band-stop filter using DGS and comb-line resonator with RF-MEMS varactors, International *Journal of Circuit Theory and Applications*, 48, 2020, pp. 1436–1449.

[57]. Mirebrahimi, Seyyed Mehdi, Massoud Dousti, and Saeid Afrang. MEMS tunable filters based on DGS and waveguide structures: a literature review, *Analog Integrated Circuits and Signal Processing*, Vol. 108, No 1, 2021, pp. 141-164.

---